Intermetallics 131 (2021) 107086

Contents lists available at ScienceDirect

Intermetallics

journal homepage: http://www.elsevier.com/locate/intermet

Screening for O phase in advanced γ–TiAl alloys

Marcus Willi Rackel *, Andreas Stark, Heike Gabrisch, Florian Pyczak

Helmholtz-Zentrum Geesthacht, Centre for Materials and Costal Research, Max-Planck-Straße 1, 21502, Geesthacht, Germany

ARTICLE INFO

Keywords:
TiAl alloys
Orthorhombic phase
Phase formation
High-energy X-ray diffraction
Rietveld refinement

ABSTRACT

This is a screening study using high-energy X-ray diffraction measurements to determine whether an orthorhombic phase forms in γ-based TiAl alloys of different compositions. The 13 alloy compositions investigated were chosen to be either close to commercial alloys or to identify the effects of different single alloying elements on the formation of orthorhombic phase. The orthorhombic O phase with Cmcm structure was found in several of those γ-TiAl alloys after an aging heat treatment at 550 °C for 20 h. The presence of different β-stabilising elements such as niobium, tantalum, molybdenum or vanadium did promote the formation of orthorhombic phase, while micro alloying elements such as carbon or boron were neutral in this respect. Furthermore, a limit for aluminium was also found, below which the orthorhombic O phase is formed in the alloys investigated. This limit lies between 46 at.% and 47 at.%.

1. Introduction

In γ-based TiAl alloys β-stabilising elements such as niobium, molybdenum or vanadium, or minor alloying elements such as carbon, silicium or boron are added to improve the mechanical properties, oxidation resistance or processability [1]. Alloying has the consequence that not only these properties are improved, but also the phase constitution and transition temperatures of the major phases can significantly change [2]. It is also possible that new phases or phases previously only known from "classical" titanium alloys form. Examples are the formation of the ordered ω_o phase with a $B8_2$ structure from the ordered β_o phase with a B2 structure [3] and the formation of the aforementioned ω_o phase from the hexagonal α_2 phase (Ti_3Al) with a $D0_{19}$ structure [4]. The formation of the orthorhombic O phase, which has been known from α_2-based titanium alloys since the late 1980's, is considered positive, in particular for the ductility of the alloy [5,6].

Recently, the formation of an orthorhombic phase that is structural similar to the O phase with a Cmcm structure was reported by Rackel et al. [7] and Gabrisch et al. [8] in a high-niobium containing γ-based TiAl alloy. However, the chemistry of that O phase differs from the ideal stoichiometric composition Ti_2AlNb. It was shown by the use of in situ high-energy X-ray diffraction (HEXRD) and high-resolution HAADF--STEM investigations that the orthorhombic O phase forms out of the hexagonal α_2 phase with a $D0_{19}$ structure in the Ti-42Al-8.5Nb alloy (all compositions in at.%). It has been found that the formation of the O phase is reversible and takes place at temperatures below 700 °C by small lattice displacements followed by a local chemical reordering achieved by changes of the site occupancy [7,8]. The emergence of the O phase is clearly evident in XRD or HEXRD measurements by the splitting of former α_2 20-20 and α_2 20-21 peaks. If both phases (α_2 phase and O phase) are represented in the lowest common crystallographic space group i.e. Cmcm, as shown in Ref. [7], then splitting can be explained by small changes of the a and b lattice parameters from $b=\sqrt{3}\cdot a$ in the α_2 phase to $b<\sqrt{3}\cdot a$ in the O phase. The detection of the O phase by TEM studies is also possible as shown by Gabrisch et al. [8] and Ren et al. [9,10]. The increasing evidence for orthorhombic phase formation in γ-based TiAl alloys requires a systematic investigation if their formation is a common phenomenon in γ-TiAl alloys. HEXRD measurements are a powerful analysis tool to gain qualitative and quantitative results on phase constitution with good grain statistics in a short time [11]. As a first step, 13 γ-based and technically relevant TiAl alloys in the composition range Ti-(42–48)Al-(0.1–10)X (X = one or more elements of Nb, Mo, Mn, V, Ta, Cr, C, B, Si) were investigated in this study (Table 1). An initial screening for the presence of an orthorhombic phase was performed with HEXRD measurements before and after an aging heat treatment at 550 °C for 20 h. The parameters for the heat treatment were taken from previous studies on the alloy Ti-42Al-8.5Nb in Ref. [7].

2. Materials and methods

The investigated alloys were produced by three different methods (Table 1): either powder metallurgy (PM), casting or casting and hot

* Corresponding author.
E-mail address: marcus.rackel@hzg.de (M.W. Rackel).

https://doi.org/10.1016/j.intermet.2021.107086
Received 8 October 2020; Received in revised form 3 December 2020; Accepted 4 January 2021
Available online 5 February 2021

extrusion.

The PM alloys were produced by Electrode Induction Melting Gas Atomization (EIGA) or by Plasma Melting Induction Guiding Gas Atomization (PIGA) [12]. The atomized powders with a particle size <180 μm were filled into cylindrical titanium capsules and compacted by hot isostatic pressing (HIP). Alloys no. 6, no. 7, no. 9 and no. 13 were produced in a modified cold crucible arc furnace from pure elements (at least 99.95 %) under an argon atmosphere (Ar 99.999 %). They are identified as "cast" in Table 1. An additional homogenisation heat treatment at 1100 °C for 168 h in air was performed on all cast samples. The alloy no. 5 was produced by vacuum arc re-melting (VAR) and hot extrusion. The ingot was capsuled and hot extruded at 1230 °C with a reduction ratio of 8:1.

All investigated samples were cut to a sample thickness of 5.0 mm. The material was annealed in a high-temperature furnace in air. The temperature was controlled by a type S thermocouple positioned near the specimens. All specimens (two specimens for each composition) were held at 700 °C for 5 h and subsequently air cooled (heat treatment A and named reference state). After heat treatment A a second heat treatment (heat treatment B) was performed with the respective second samples at 550 °C for 20 h followed by subsequent furnace cooling. The samples were measured with HEXRD in both heat treatment conditions.

The HEXRD experiments were performed at the Helmholtz-Zentrum Geesthacht (HZG) run High Energy Materials Science beam line (HEMS) at PETRA III at the Deutsches Elektronen-Synchrotron (DESY), Hamburg, Germany [13]. The measurements were performed at room temperature, in transmission using a beam size of 0.5 mm by 0.5 mm and a photon energy of 87.1 keV (λ=0.14235 Å). During the HEXRD, experiments the Debye-Scherrer diffraction rings were recorded on a Perkin Elmer XRD 1621 flat panel detector. An exposure time of 0.2 s was used and 20 images were collected and summed up for each specimen to increase the dynamic range of the detector. In order to determine the instrumental parameters, beam centre and the sample-detector distance, a calibration measurement using a lanthanum hexaboride (LaB_6) powder standard was performed [14]. The phase fractions and lattice parameters were calculated using the Rietveld analysis software package MAUD [15]. The crystallographic structures and phases used in these calculations are described in Ref. [7].

3. Results and discussion

The results of the diffraction measurements are shown in Table 1 and in Figs. 1 and 2.

Fig. 1(a) shows the diffraction pattern from the Ti-42Al-8.5Nb alloy (alloy no. 1) obtained by HEXRD, and compares the main diffraction peaks of the alloy in the two different heat treated conditions heat-treatment A state (reference state, black) and heat-treatment B state, 550 °C/20 h/AC (red). In Fig. 1(b) an enlarged section of the dashed box in Fig. 1(a) is shown. There, the splitting of the former α_2 20-20 diffraction peak due to the formation of an orthorhombic phase is clearly visible after heat treatment at 550 °C/20 h/AC. A detailed description and discussion of the observations made follows. In Fig. 2 all investigated alloy compositions and their diffraction patterns after heat-treatment A and heat-treatment B are presented. The heat-treatment A state (reference state) is marked in black. The changes of the diffraction patterns caused by heat-treatment B are marked in red.

Niobium is one of the most commonly used alloying elements in γ-TiAl alloys to optimise the high-temperature creep [1,16] and oxidation resistance [17,18]. Simultaneously, alloying with niobium strongly influences the phase constitution and transition temperatures and importantly, it is a pre-requisite for the formation of the O phase. Certain amounts of niobium, or other β-stabilising elements with a corresponding niobium equivalent, are required to form O phase. The initial orthorhombic distortion of the hexagonal unit cell is evident from a slight broadening at the base of the α_2 20-20 and α_2 20-21 diffraction peaks.

In previous publications of Appel et al. [16,19,20] the formation of the orthorhombic B19 phase has been discussed in the Ti-42Al-8.5Nb alloy. These results could not be confirmed by the studies conducted here. Already in Ref. [7] it could be shown by the authors by a comparison of simulated crystal structures of both possible phases (B19 and O phase) with HEXRD measurements, that for the O phase there is a significantly better positional agreement of individual phase peaks and a lower total deviation between the simulated crystal structure and real measurement than for B19 phase. When evaluating diffractograms, a good agreement of peak positions and peak heights is a clear indication for the presence of a certain phase or crystal structure. The main difference between the B19 phase and the O phase is the site occupancy of the Wyckoff positions 4c1 and 4c2. The site occupancy strongly influences the electron density and leads to changes in the diffractogram. Where the site occupancy of 4c1 and 4c2 positions in the B19 phase should be identical, the O phase has different site occupancies [7].

Furthermore, the presence of the O phase in the Ti-42Al-8.5Nb alloy could be clearly proven by TEM analysis by Gabrisch et al. [8]. For other compositions with higher aluminium concentrations it was proven by Ren et al. [9,10]. Both authors agree that the orthorhombic phase formed is the O phase and not the B19 phase. It is important to note that the O phase investigated here does not have the stoichiometric composition Ti_2AlNb. Based on TEM studies, a chemical composition of 55 % titanium, 35 % aluminium and 10 % niobium was determined for the α_2 phase, which acts as the starting phase for the formation of the O phase. For the O phase itself, a chemical composition of 54 % titanium,

Table 1
Investigated alloys and their production route, including heat treatments. PM = powder metallurgical with PIGA or EIGA process, cast = arc melting furnace, hot extrusion = VAR and hot extrusion. The cast alloys were homogenised at 1100 °C for 168 h before any other heat treatments were performed. Additionally, the phase constitution after heat-treatment A, and the results from screening for an orthorhombic phase after heat-treatment B are presented.

number	*alloy composition (at.%)*	*production process*	*heat treatment*	*phase fraction (vol. %) in* heat-treatment *A state*			heat-treatment *B state*
				α_2	β_o/ω_o	γ	orthorhombic phase formation
1	Ti-42Al-8.5Nb	PM	A (700 °C/5 h/AC)/B (550 °C/20 h/FC)	31.2	–/7.6	61.2	yes
2	Ti-42Al-8.5Nb-0.2C	PM		43.7	–/–	56.3	yes
3	Ti-43.5Al-4Nb-1Mo-0.1B	PM		9.8	19.6/–	70.6	yes
4	Ti-44.5Al-6.25Nb-0.8Mo-0.2C	PM		7.3	11.1/–	81.6	ambiguous
5	Ti-45Al-5Nb-0.2B-0.2C	hot extrusion		9.8	–/–	90.2	no
6	Ti-45Al-4Nb-4Ta	cast		18.5	–/2.0	79.5	yes
7	Ti-45Al-4Nb-4Ta-0,2B	cast		8.5	–/4.3	87.2	yes
8	Ti-45Al-7.5Nb	PM		15.6	–/0.3	84.1	yes
9	Ti-45Al-8V	cast		14.5	14.7/–	70.8	yes
10	Ti-45Al-10Nb	PM		6.2	–/4.6	89.2	yes
11	Ti-46Al-9Nb	PM		4.7	–/–	95.3	yes
12	Ti-47Al-1.5Nb-1Mn-1Cr-0.2Si-0.5B	PM		2.0	–/–	98.0	no
13	Ti-48Al-4Nb-4Ta	cast		2.3	–/–	97.7	no

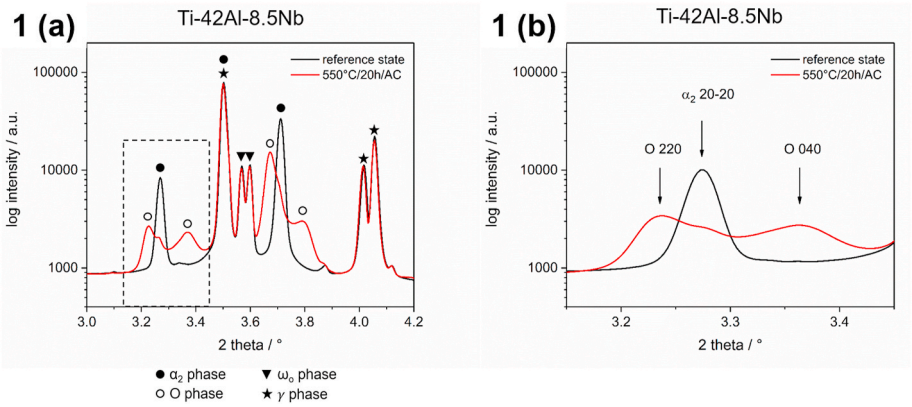

Fig. 1. Diffraction pattern from the Ti-42Al-8.5Nb alloy obtained by HEXRD. (a) Comparison of the main diffraction peaks in the two different heat treated conditions. (b) Enlarged section of the dashed box in Fig. 1(a). The splitting of the former α_2 20-20 diffraction peak (black curve, reference state) due to the formation of an orthorhombic phase is clearly visible after heat treatment at 550 °C/20 h/AC (red curve).

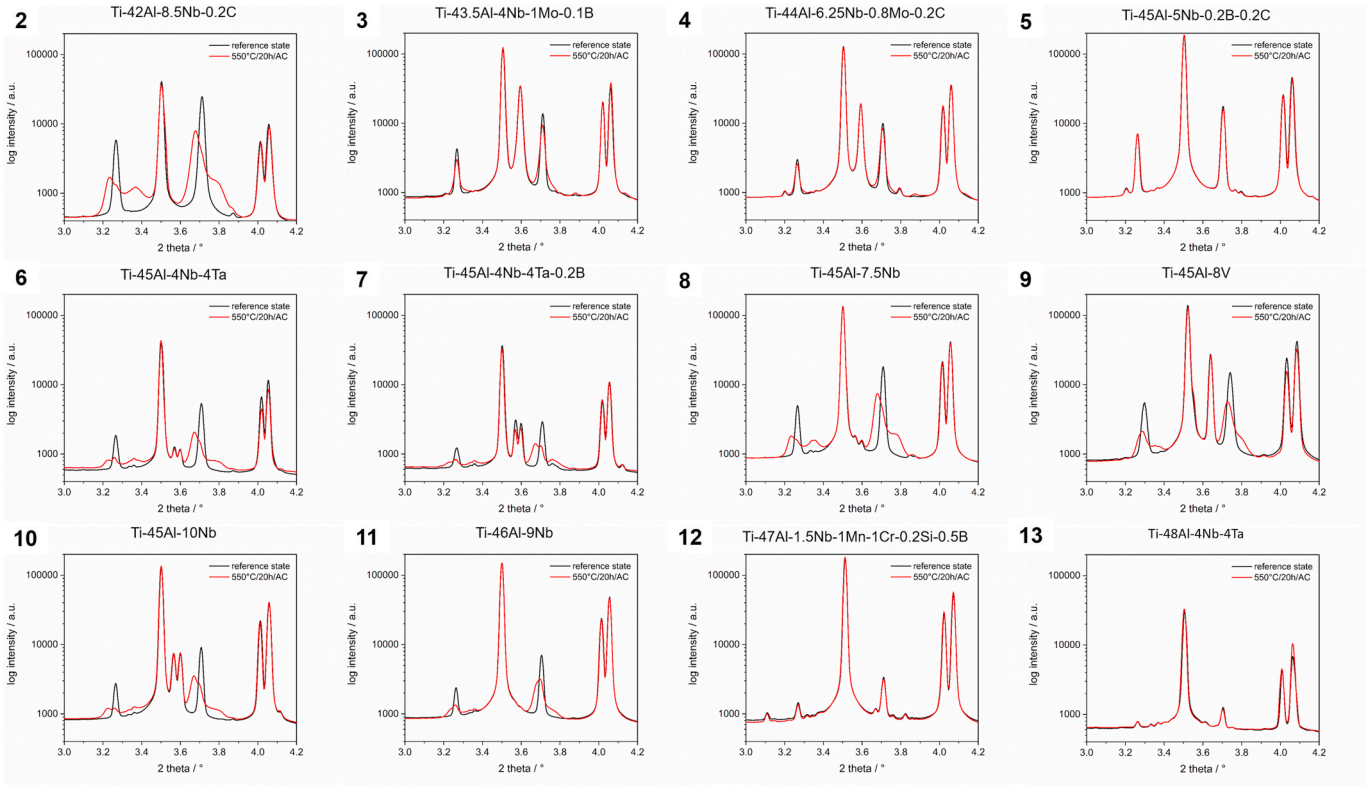

Fig. 2. HEXRD diffraction patterns obtained from the alloys investigated after heat-treatment A and heat-treatment B, the alloy compositions are indicated by the corresponding alloy numbers. For each alloy two heat treated conditions were compared. The black curve represents the reference state (heat-treatment A, 700 °C/5 h/air cooled) where no orthorhombic phase was present. The red curve indicates the heat-treatment B condition (550 °C/20 h/air cooled). This heat treatment temperature is within the temperature range for the formation of the O phase, the O phase being formed in some of the alloys investigated.

37 % aluminium and 9 % niobium was determined after an ageing time of 168 h [7] in the Ti-42Al-8.5Nb alloy.

Based on theoretical considerations, there is a further reference in the literature to the O phase that forms from the α_2 phase with $D0_{19}$ structure. Bendersky et al. [21] described in their study possible formation paths of orthorhombic phases in the Ti–Al–Nb system based on group/subgroup relationships due to changes of the site occupancy and symmetry reduction. They showed that the formation of O phase out of the α_2 phase with $D0_{19}$ structure is possible, when the α_2 phase with $D0_{19}$ structure acts as starting phase for the phase transformation. The formation of the B19 phase is possible out of the cubic ordered βo phase with B2 structure or out of the α phase with A3 structure via an orthorhombic A20 structure. A direct formation of B19 phase out of the ordered hexagonal α_2 phase with $D0_{19}$ structure is not possible.

Summarising both, the experimental results from Refs. [7–10] and the theoretical considerations [21], it can be concluded that the orthorhombic phase formed is the O phase with Cmcm structure, but does not have the ideal stoichiometric composition Ti_2AlNb. Based on these findings, the following experiments were evaluated considering the formation of the orthorhombic O phase with Cmcm structure out of the ordered hexagonal α_2 phase with $D0_{19}$ structure using the crystal structures from Ref. [7].

A threshold niobium concentration above which O phase forms becomes evident when comparing alloy no. 5 and no. 8 after heat-

treatment B. Alloy no. 8 with a niobium concentration of 7.5 at.% shows a clear splitting of the α_2 20-20 and α_2 20-21 peaks which indicates the formation of an orthorhombic phase. However alloy no. 5, with a niobium concentration of only 5 at.%, shows no signs of peak splitting. These results indicate, that the minimum concentration of niobium required for orthorhombic phase formation lies between 5 at.% and 7.5 at.%. On increasing the niobium content to 9 at.% (in alloy no. 11) and 10 at.% (alloy no. 10) the O phase can be clearly identified in the diffraction patterns at the aforementioned α_2 20-20 and α_2 20-21 peak positions and no further changes are observed after 20 h at 550 °C. The HEXRD diffraction patterns show the simultaneous presence of the α_2 and O phase. This is in line with TEM results of Gabrisch et al. [8] and Ren et al. [9,10]. In their studies on the phase morphology of the O phase, the co-existence of both phases was confirmed. Unfortunately, a quantitative analysis of the fraction of O phase and of the remaining α_2 phase using Rietveld refinement is not possible in most cases examined here. This is due to the large number of overlapping peaks from both phases. Nevertheless, an indication of the presence of remaining α_2 phase are the small shoulders between the O phase 220 and 040 peaks and the O phase 221 and 041 peaks at 2 θ angles of former α_2 20-20 and α_2 20-21 peaks. For the Ti-42Al-8.5Nb alloy (alloy no. 1, Fig. 1(b)) a rough estimation of the remaining α_2 phase was made, based on a Gaussian and Bigaussian fit of the integral intensity of single α_2 phase peaks using the OriginPro 2017 software tool. For this, the integral intensity of the α_2 20-20 peak (Fig. 1(b), black curve) in heat-treatment A state was compared to the integral intensity in heat-treatment B condition (red curve). Based on the Rietveld refinement of the heat-treatment A state, the α_2 phase fraction in this heat treatment state was determined to be 31.2 % (Table 1). In the heat-treatment B state, the α_2 20-20 peak intensity is reduced at the expense of the newly formed O phase to an estimated retained α_2 phase fraction of 5.5 %. In other words, after 20 h at 550 °C over 80 % of the α_2 phase has transformed to an orthorhombic phase.

Other β-stabilising alloying elements may substitute for niobium with respect to stabilising the O phase. This is evidenced by alloys no. 6 and no. 7 which have a tantalum and niobium concentration of 4.0 at.% each. Here, the O phase forms even though the amount of niobium is below the threshold level reported above for Ti–Al–Nb alloys.

Two molybdenum containing alloys were investigated, alloy no. 3, known as TNM and no. 4 known as TNB-V4. In both alloys the niobium content is reduced and was partly replaced by molybdenum to balance properties [2]. As indicated in Fig. 2, a clear orthorhombic splitting of former α_2 20-20 and α_2 20-21 diffraction peaks is not visible. Only slight broadening at the base of the peaks is visible, indicating the initial stages of an orthorhombic distortion of the α_2 crystal structure. This assumption is supported the fact that there are no changes in the peak height of the other major phases γ and β_o. Furthermore, no other microstructural changes are expected to happen at 550 °C. A significant grain refinement of the α_2 phase, which could also cause such peak broadening, was not observed in the HEXRD pattern. Recent HEXRD measurements by Rittinghaus et al. [22] however, support the observation that O phase may form in the TNM alloy. The HEXRD measurements carried out in this work show clear signs of O phase formation. Additionally, Musi et al. [23] observed in a Ti-44.5Al-3.2Mo-0.1B alloy the formation of an orthorhombic phase as an intermediate or transition phase during heating of β quenched samples.

Alloy no. 9 with a vanadium content of 8.0 at.% also shows signs of the orthorhombic phase after heat-treatment B. This is apparent from splitting of the former α_2 20-20 and α_2 20-21 diffraction peaks. Thus vanadium additions can also favour the formation of an orthorhombic phase. This finding is new, and contradicts the database of the Ti–Al–V phase diagram by Thermo-Calc Software AB in data base TCS Ti/TiAl-based Alloys Thermodynamic Database (TCTI, V2.0) [24]. There, the presence of an orthorhombic phase is not found. In a direct comparison with alloy no. 8, that contains 7.5 at.% niobium, the orthorhombic splitting of the former α_2 20-20 and α_2 20-21 diffraction peaks is less pronounced in the Ti–Al–V alloy. The reason for this is not yet known, but different formation energies for the O phase as well as different formation temperatures compared with the Ti–Al–Nb system could be factors. Further investigations on this are necessary and ongoing. Carbon is known as a strong α_2 and α stabilising alloying element. In the alloys no. 2, 4 and 5 studied (0.2 at.% C), no signs of carbides were found in the diffractograms. This indicates that the addition of 0.2 at.% carbon is below the solubility limit here. However, the α_2 stabilising effect of carbon becomes apparent by comparing the change in phase constitution between alloys no. 1 and no. 2 (0.2 at.% C). In the reference state (heat-treatment A), alloy no. 1 consists of the α_2, ω_o and γ phases, whereas in alloy no. 2 no signs of the ordered β_o phase or ω_o phase were found (Table 1). After heat-treatment B the O phase forms in both alloys at the expense of the α_2 phase, but some α_2 phase still remains. Based on the comparison of the intensity of the remaining α_2 20-20 peaks in heat-treatment B state to that of the reference state we find that comparable proportions of O phase have formed from α_2 phase in alloys no. 1 and 2. Therefore, we conclude that the addition of carbon does not influence the amount of O phase formed out of the α_2 phase.

The addition of small amounts of boron to alloy no. 7 leads to no significant change in the phase constitution compared to alloy no. 6 where no boron was added. After heat-treatment B the O phase is present in both alloys. However the diffractogram of alloy no 7 shows nearly continuous Debye-Scherrer diffraction rings, which indicates a fine grained microstructure. For comparison, the alloy without boron exhibits spotty rings with coarse reflections originating from a few larger grains. The refining effect of boron additions is also visible in alloys no.3, no.5 and no. 12. One can conclude that the addition of 0.1–0.5 at. % of boron did not influence the amount of O phase formed.

Aluminium is the alloying element with the most significant influence on the phase constitution and solidification path of TiAl alloys. Referring to the binary TiAl phase diagram [25], a reduction of the aluminium content automatically leads to a higher content of α_2 phase and thus to increased volume fraction of the starting phase from which the O phase forms, $\alpha_2 \rightarrow$ O. In the composition range 42–46 at.% aluminium and with a sufficiently high amount of β-stabilising alloying elements, the formation of the O phase was observed. For an aluminium content of 47 at.% and above (alloys no. 12 and 13), no signs of orthorhombic phase were observed, despite a comparable amount of β-stabilising elements as in alloys no. 6 and no. 13. These observations lead to the conclusion, that apart from a minimum amount of β-stabilising elements, there is also a limit to the aluminium content above which the orthorhombic phase does not form. Based on the presented experimental results, this limit lies between 46 at.% and 47 at.% of aluminium. Based on the current observations, it cannot yet be determined whether the absence of the O phase is due to a change in the solidification path in the alloy or due to the higher aluminium concentration corresponding to lower amount of α_2 phase (about 2 %), which is the starting phase for the phase transformation $\alpha_2 \rightarrow$ O. To answer these questions, detailed investigations in the transition area would be necessary.

4. Conclusions

In the present study, HEXRD experiments were performed to show, that in γ-TiAl based alloys in the composition range Ti-(42–48)Al-(0.1–10)X (X = one or more elements of Nb, Mo, Mn, V, Ta, Cr, C, B, Si) an orthorhombic phase with Cmcm structure can form after aging heat treatment at 550 °C for 20 h. Alloying with Nb, Mo, Ta, V, shows that either a minimum amount of a single element or a combination of alloying elements above a specific threshold can cause an orthorhombic phase formation in TiAl alloys. Exact details on each element or combinations thereof were not the topic of this study. For Nb the threshold lies between 5 and 7.5 at.%, The finding of O phase for alloying with V is new. For aluminium a limit was also found, below which the orthorhombic O phase is formed in combination with a sufficiently high

amount of β-stabilising elements. This limit lies between 46 at.% and 47 at.%.

Minor (interstitial) alloying elements like carbon or boron did not influence the amount of orthorhombic phase formed.

Author statement

Dr. Marcus W. Rackel: Conceptualization, Methodology, Validation, Investigation, Formal analysis, Writing Original Draft, Visualization.

Dr. Andreas Stark: Investigation, Writing Review and Editing.

Dr. Heike Gabrisch: Writing Review and Editing.

Prof. Dr. Florian Pyczak: Writing Review and Editing.

Declaration of competing interest

The authors declare that they have no known competing financial interests or personal relationships that could have appeared to influence the work reported in this paper.

References

[1] F. Appel, J.D.H. Paul, M. Oehring, Gamma Titanium Aluminide Alloys, Wiley-VCH, 2011.
[2] H. Clemens, S. Mayer, Adv. Eng. Mater. 15 (4) (2013) 191–215.
[3] A. Stark, M. Oehring, F. Pyczak, A. Schreyer, Adv. Eng. Mater. 13 (8) (2011) 700–704.
[4] L. Song, X. Xu, L. You, Y. Liang, Y. Wang, J. Lin, Acta Mater. 91 (2015) 330–339.
[5] D. Banerjee, A.K. Gogia, T.K. Nandi, V.A. Joshi, Acta Metall. 36 (4) (1988) 871–882.
[6] F. Chu, T.E. Mitchell, B. Majumdar, D. Miracle, T.K. Nandy, D. Banerjee, Intermetallics 5 (2) (1997) 147–156.
[7] M.W. Rackel, A. Stark, H. Gabrisch, N. Schell, A. Schreyer, F. Pyczak, Acta Mater. 121 (2016) 343–351.
[8] H. Gabrisch, U. Lorenz, F. Pyczak, M. Rackel, A. Stark, Acta Mater. 135 (2017) 304–313.
[9] G.-d. Ren, C.-r. Dai, W. Mei, J. Sun, S. Lu, L. Vitos, Acta Mater. 165 (2019) 215–227.
[10] G.-d. Ren, J. Sun, Acta Mater. 144 (2018) 516–523.
[11] K.-D. Liss, A. Bartels, A. Schreyer, H. Clemens, Textures Microstruct. 35 (3–4) (2003) 219–252.
[12] R. Gerling, H. Clemens, F.P. Schimansky, Adv. Eng. Mater. 6 (1–2) (2004) 23–38.
[13] N. Schell, A. King, F. Beckmann, T. Fischer, M. Müller, A. Schreyer, Mater. Sci. Forum 772 (2014) 57–61.
[14] D.R. Black, D. Windover, A. Henins, J. Filliben, J.P. Cline, Standard Reference Material 660B for X-Ray Metrology, National Institute of Standards and Technology, Gaithersburg, 2010, pp. 140–148.
[15] L. Lutterotti, Nucl. Instrum. Methods Phys. Res. Sect. B Beam Interact. Mater. Atoms 268 (3–4) (2010) 334–340.
[16] F. Appel, J.D.H. Paul, M. Oehring, Mater. Sci. Eng.: A 510– 511 (2009) 342–349, 0.
[17] S. Taniguchi, T. Shibata, Intermetallics 4 (Supplement 1) (1996) S85–S93.
[18] J.P. Lin, L.L. Zhao, G.Y. Li, L.Q. Zhang, X.P. Song, F. Ye, G.L. Chen, Intermetallics 19 (2) (2011) 131–136.
[19] F. Appel, M. Oehring, J.D.H. Paul, Adv. Eng. Mater. 8 (5) (2006) 371–376.
[20] F. Appel, M. Oehring, J.D.H. Paul, Mater. Sci. Eng., A 493 (1–2) (2008) 232–236.
[21] L.A. Bendersky, A. Roytburd, W.J. Boettinger, Acta Metall. Mater. 42 (7) (1994) 2323–2335.
[22] S.K. Rittinghaus, J. Schmelzer, M.W. Rackel, S. Hemes, A. Vogelpoth, U. Hecht, A. Weisheit, Materials 13 (19) (2020).
[23] M. Musi, P. Erdely, B. Rashkova, H. Clemens, A. Stark, P. Staron, N. Schell, S. Mayer, Mater. Char. 147 (2019) 398–405.
[24] T.-C.S. AB, TCTI2: TCS Ti/TiAl-Based Alloys Database, Thermo-Calc Software AB, Solna, Sweden, 2019.
[25] J.C. Schuster, M. Palm, J. Phase Equilibria Diffus. 27 (3) (2006) 255–277.